Structural and Magnetic Relaxation of $Fe_{61}Co_{10}Y_8Mo_1B_{20}$ Bulk Amorphous Alloy Obtained Using Two Methods

PAWEL PIETRUSIEWICZ*, MARCIN NABIALEK, BARTLOMIEJ JEZ
Institute of Physics, Czestochowa University of Technology, 19 Armii Krajowej Av., 42-200 Czestochowa, Poland

Bulk amorphous $Fe_{61}Co_{10}Y_8Mo_1B_{20}$ alloys in the form of plates have been prepared using two methods: suction casting and injection casting. The structure of the as cast samples have been studied using Mossbauer spectroscopy. The obtained Mossbauer spectra are typical for materials of amorphous structure. In the hyperfine field distributions obtained from the Mossbauer spectra analysis, there are variations between the probability of occurrence of magnetic atoms around central atom. Then, magnetic susceptibility disaccommodation has been measured for the tested samples. These measurements indicate that the structural relaxation in the studied samples occur at the elementary level. Injection casting method for the tested alloy determines, in the material volume, the formation of more point relaxators in the form of free volume.

Keywords: bulk amorphous alloys, disaccommodation, Mossbauer spectroscopy

Amorphous alloys are one of the newest groups of metallic materials. The materials in this group are characterized by exceptional properties, significantly exceeding those that have commercially produced crystalline alloys. Generally, amorphous materials can be divided into classical and massive ones. This division is related to their thickness. Classic amorphous alloys are produced in the form of strips with a thickness of a dozen or a hundred micrometers, whereas massive amorphous alloys have a thickness much greater than one hundred micrometres [1-3].

Depending on the alloy manufacturing method, the change in their properties is observed. It is expected that this is associated with a change in the cooling rate, which in the case of the amorphous tape manufacturing process can be from 10^4 - 10^6 K/s, and for massive amorphous alloys is in the range 10^{-1} - 10^3 K/s. With such differences in the cooling rate, it is easy to infer its impact on the properties of the products. If we describe massive amorphous materials produced at similar cooling rates, the description of their properties becomes much more difficult.

Due to the structure of the amorphous alloy itself and the chemical composition, they may show a higher corrosion resistance much higher microhardness parameter, greater resistance to mass loss, low coercivity field, high saturation magnetization in comparison with their crystalline counterparts [4-18]. The typical parameters described above are for amorphous ferromagnetic alloys based on FeCoB exhibiting so-called soft magnetic properties [19].

As shown by the results of research in [20-22], the structural stresses associated with the so-called relaxators. The influence of structure stresses on magnetic properties can be investigated using two methods. One method is related to the analysis of the temporal change in the initial magnetic susceptibility in the Rayleigh area [23-25]. The second one is based on the analysis of the curves of the primary magnetization in high magnetic fields above the effective anisotropy field [26-27]. Both theories are adapted by H. Kronmuller to indirectly investigate the influence of structural defects on the magnetization process. The use of these theories gives the opportunity to describe the real structure of the studied alloys, and to describe the phenomena occurring in them.

In this work we have studied $Fe_{61}Co_{10}Y_8Mo_1B_{20}$ alloy In this work we have studied $Fe_{61}Co_{10}Y_8Mo_1B_{20}$ alloy made by two methods with similar cooling rate.

Theoretical basics

The disaccomodation of magnetic susceptibility is one of the phenomena of magnetic delay occurring during the magnetization of amorphous ferromagnetic materials in the magnetic field in the Rayley area. The disaccomodation of the initial magnetic susceptibility is related to its decrease in time from the moment of demagnetization of the sample and is calculated in accordance with the relation [28-30]:

$$\Delta\left(\frac{1}{\chi}\right) = \frac{1}{\chi(t_2)} - \frac{1}{\chi(t_1)} \qquad (1)$$

where:

$\chi(t_1)$ and $\chi(t_2)$ are the values of magnetic susceptibility measured in 2 s and 120 s after demagnetizing the sample with alternating current with an amplitude falling to zero

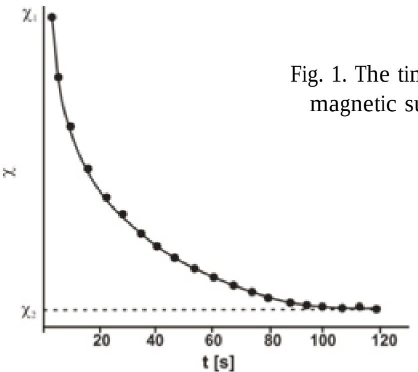

Fig. 1. The time dependence of magnetic susceptibility [31]

The described effect of the magnetic delay is related to the change in the orientation of the axis orientation of the atomic pairs in the domain walls near free volumes [28, 29].

The decrease in magnetic susceptibility during the time of demagnetization of the sample is related to the change in the orientation of atomic pairs (fig.2), which tend to set their axes according to the direction of spontaneous

---

* email: pietrusiewicz.pawel@wip.pcz.pl

magnetization. The directional orientation of these axes affects the distribution of local anisotropy and, consequently, deepening the well of the domain wall stabilization potential (fig. 3) [32-36]

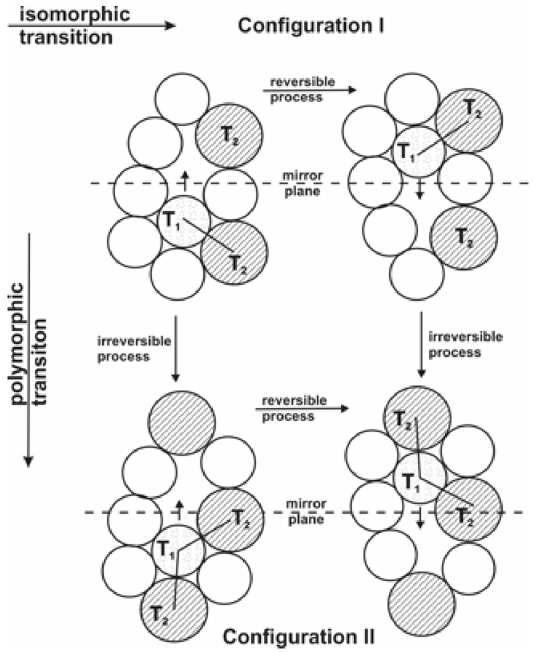

Fig. 2. A model of rigid balls showing two orientations of the axis of atomic pairs, corresponding to two energy levels and representing reversible and irreversible relaxation processes [29, 34]

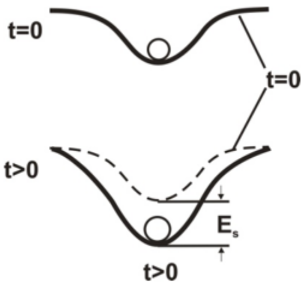

Fig. 3. Establishment of the domain wall stabilization potential in time [29]

Experimental part

Samples of $Fe_{61}Co_{10}Y_8Mo_1B_{20}$ made from high purity components above 99.9%. The research material was obtained in two stages. The first stage was the preparation of polycrystalline ingots that consisted in melting the alloy components. This process was carried out in an arc furnace under a protective atmosphere of argon. Samples for testing in the form of plates were produced using two methods: injection method and the method of aspirating a liquid alloy into a copper mold. In both cases, the process was carried out under a protective atmosphere of argon. The samples thus obtained were subjected to structure analysis using the X-ray diffraction. The Bruker model Advance D8 XRD diffractometer was used (Cu-K_α). The samples were irradiated in the angle range 2θ 30°-100° with an exposure time of 5 s per measuring step of 0.02 °. The structure of alloys was also tested using Mossbauer transmission spectroscopy (POLON 2330). The spectrometer worked on a 57Co (Rh) source with 50 mCi activity.

The disaccomodation of the initial magnetic susceptibility were measured using automated apparatus in which the transformer method is used. Samples in the form of plates were placed in a yoke made of a superpermalve in a vacuum tube. The disaccomodation tests of the initial magnetic susceptibility were carried out in the temperature range from room temperature to the temperature exceeding the Curie temperature (T_c).

The numerical analysis of magnetic disaccomodation curves as a function of temperature was made for the distribution of the continuous spectrum of relaxation times [30]:

$$\Delta\left(\frac{1}{\chi}\right) = \sum_{i=1}^{l} \int_{-3\beta_{\tau i}}^{+3\beta_{\tau i}} \beta_\tau^{-1} \pi^{-1/2} \frac{I_{pi} T_{pi}}{T} \left(e^{-t_1/\tau_{mi} e^z} - - e^{-t_2/\tau_{mi} e^z}\right) e^{-(z/\beta_{\tau i})^2}\, dz \qquad (2)$$

where:

T_{pi} - maximum temperature of disaccomodation
I_{pi} - the intensity of the *i*-th process at temperature
Q_{mi} – average activation energy
β_τ - width of the distribution

Mean relaxation time t_{mi} is given by:

$$\tau_{mi} = \tau \exp\left(-\frac{Q_{mi}}{k}\left(\frac{1}{T} - \frac{1}{T_{pi}}\right)\right) \qquad (3)$$

Results and discussions

Figure 4 presents X-ray diffractograms measured for $Fe_{61}Co_{10}Y_8Mo_1B_{20}$ alloy samples in the state after solidification produced by two methods: forcing and sucking the liquid alloy into a copper water cooled mold. Both diffractograms shown in figure 3 are similar and consist only of a wide fuzzy maximum in the angle of 2θ from 40 to 50°.

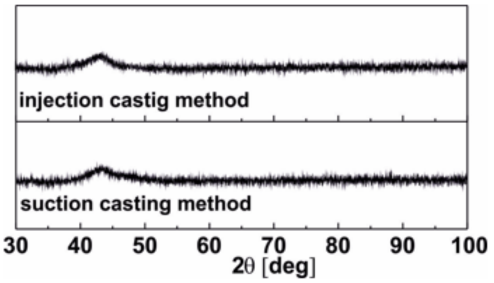

Fig. 4. XRD diffractograms for $Fe_{61}Co_{10}Y_8Mo_1B_{20}$ alloy samples in the form of plates produced using two methods.

Such diffractograms are characteristic of amorphous materials in which there is no long-range atomic arrangement.

Figures 5 and 6 show the Mossbauer spectra measured in transmission symmetry at room temperature and the corresponding hyperfine field distributions B_{hf} on the ^{57}Fe nuclei. The spectra shown in figures 5a and 6a are wide and asymmetrical which is characteristic of amorphous materials.

The hyperfine field distributions obtained from the numerical analysis of the Mossbauer transmission spectra and the ^{57}Fe nuclei are bimodal. It means that in the volume of produced samples without division into the method of obtaining them, there are areas with different concentrations of Fe. The low- and high-field components are clearly visible in these distributions. This shape of hyperfine index distributions on ^{57}Fe nuclei means that there are more or less iron rich areas in the material volume. This means that there are many possible configurations of the closest magnetic neighbors around the Fe central atom. It mainly concerns Fe-Fe, Fe-Co and Co-Co pairs. It should also be taken into account that the surroundings of atoms can change stochastically [33]. The results of spectra analysis are presented in table 2.

Figure 7 shows the temperature dependence of the initial magnetic susceptibility for the alloy produced by various

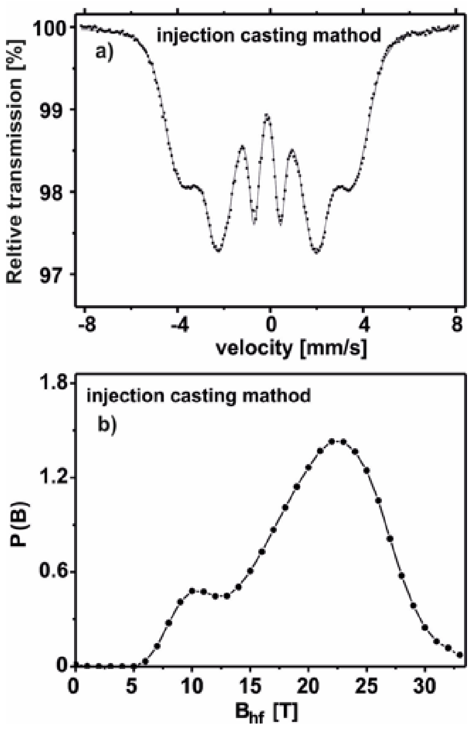

Fig. 5. Transmission Mössbauer spectrum (a) and the corresponding hyperfine field distribution on ^{57}Fe nuclei (b) obtained for $Fe_{61}Co_{10}Y_8Mo_1B_{20}$ alloys prepared using the method of injecting a liquid alloy into a copper liquid-cooled form

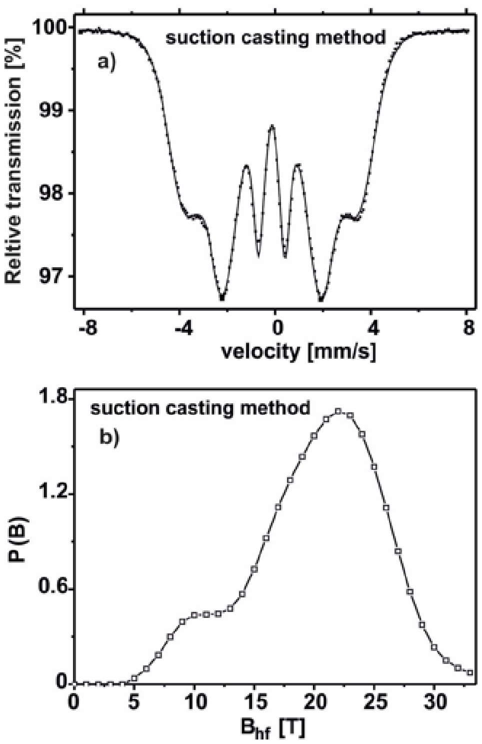

Fig. 6. Transmission Mossbauer spectrum (a) and the corresponding hyperfine field distribution on ^{57}Fe nuclei (b) obtained for $Fe_{61}Co_{10}Y_8Mo_1B_{20}$ alloys prepared using the method of aspirating a liquid alloy into a copper liquid-cooled form

Table 1

THE VALUE OF THE HYPERPHINE FIELD USING THE ^{57}Fe NUCLEI (B_{ef}) AND DISPERSION OF THE HYPERFINE FIELD DISTRIBUTIONS OF THE AMORPHOUS PHASE (D_{am}) *(<$A_{2,5}$>)*

Sample	B_{ef} [T]	D_{am} [T]	<$A_{2,5}$>
Injection casting	20.38 (0.048)	5.694 (0.049)	2.05819 (0.05)
Suction casting	20.21 (0.03)	5.446 (0.027)	2.19923 (0.022)

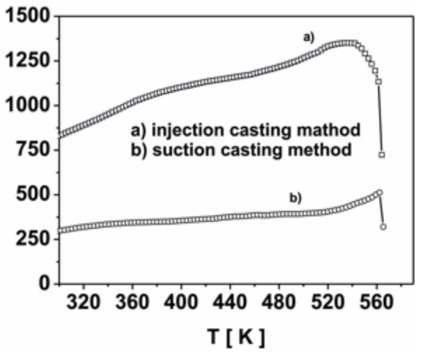

Fig. 7. Temperature dependence of the initial magnetic susceptibility for the alloy $Fe_{61}Co_{10}Y_8Mo_1B_{20}$ in the form of: a plate manufactured by pressing and produced by suction casting

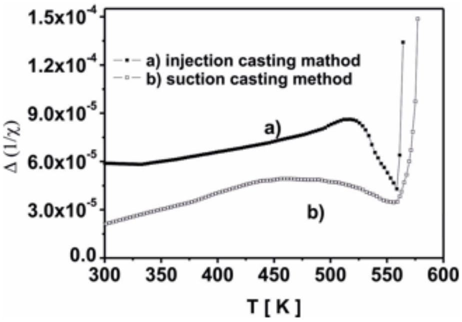

Fig. 8. Isochronous distortion curves of magnetic susceptibility for the alloy $Fe_{61}Co_{10}Y_8Mo_1B_{20}$ in the form of: a plate prepared by pressing and a plate produced by suction method

methods. the course of initial magnetic susceptibility to a temperature of approx. 500K for both samples is similar. Change in the course of the initial vulnerability as a function of temperature is visible in the area of the ferro-to-paramagnetic transition. A gentle ferro-pramagnetic passage is observed for the sample prepared by the injection method, whereas for the sample produced by the suction method this transition is associated with a rapid drop. This behavior of the curves of the initial magnetic susceptibility is associated with close range stresses of the magnetic structure. It is clearly visible that the more homogeneous magnetic structure appears in the alloy produced by the suction method. These results should be linked to the Mossbauer studies (fig. 6b). Lack of clarity between low and high field components indicates a reduced number of different environments around the central atom.

Figure 8 contains isochronous curves of magnetic susceptibility to the tested alloy $Fe_{61}Co_{10}Y_8Mo_1B_{20}$ produced using two production methods.

The disaccomodation of the initial magnetic susceptibility as mentioned before is associated with relaxation processes within the so-called free volumes. Curve shape $(\Delta(1/\chi))(T)$ is an indirect measure of sample relaxation. In the case of the injection molded sample, a constant increase is observed to a temperature close to the Curie temperature, which may suggest that there are many different configurations of Fe atoms in the sample volume. However, in the case of a sample generated by suction on the curve in the range up to approximately 470 K, its increase occurs, which should be explained as above. A decrease above 475 K indicates that the sample of the $Fe_{61}Co_{10}Y_8Mo_1B_{20}$ alloy produced by

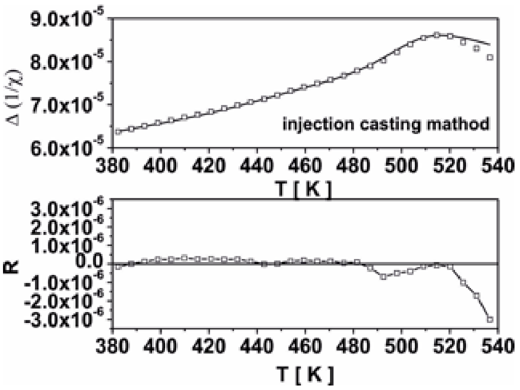

Fig. 9. Theoretical isochronatic curve of disaccomodation of the magnetic susceptibility of the plate produced by the injection method

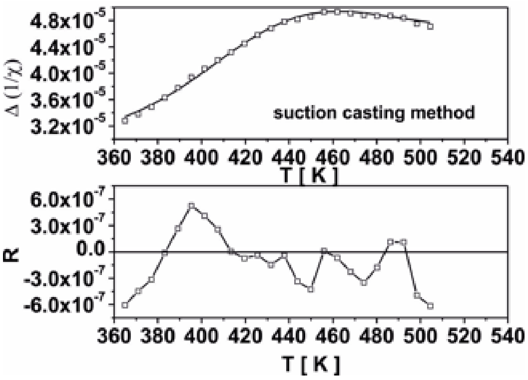

Fig. 10. Theoretical isochronic curve of disaccomodation of magnetic susceptibility of the plate produced by suction casting

Table 2

PARAMETERS OBTAINED FROM FITTING OF ISOCHRONAL DISACCOMMODATION CURVES FOR THE AMORPHOUS $Fe_{61}Co_{10}Y_8Mo_1B_{20}$ ALLOYS IN THE AS-QUENCHED STATE

Sample	Process	T_p [K]	I_p	Q_m [eV]	$\tau\ 10^{-15}$ [s]
Injection casting	I	430	$3{,}74\ 10^{-6}$	1,39	1,12
	II	475	$6.63\ 10^{-6}$	1,50	2,95
	III	518	$1{,}23\ 10^{-5}$	1,63	3,69
Suction casting	I	430	$5{,}82\ 10^{-6}$	1,33	6,54
	II	455	$1{,}29\ 10^{-5}$	1,41	6,98
	III	-	-	-	-

suction is much more relaxed than the sample produced by the injection method. For the studied alloy, Hopkinson's peak was observed regardless of the method of production [25].

Using the relationship (2), the theoretical curves of magnetic susceptibility to disaccomodation with superimposed experimental points were determined (figs. 9 and 10) and the distribution of R deviations between the theoretical curve and the experimental points.

Curve matching parameters $(\Delta(1/\chi))(T)$ are summarized in table 2.

Based on the analysis of the data collected in table 2, it can be concluded that the relaxation processes occurring in the tested alloy without taking into account the production method are related to reorientation of the atomic pairs near free volumes acting as relaxants. The range of energy for the activation of elementary processes and the order of the in Arrhenius law is consistent with the *t* ratio and assumptions of Kronmuller's theory for amorphous materials.

Conclusions

Using the methods of: sucking in and inserting a liquid alloy into a copper liquid-cooled form, it is possible to obtain massive amorphous materials in the form of 0.5 mm thick plates (confirmed by the Mossbauer and XRD tests).

Based on the distributions of hyperfine fields on the Fe57 nuclei it was found that a clear transition between the low and high nucleus components influences the dependence of the initial magnetic permeability as a function of temperature and its disaccomodation of figure 5b and figure 6b, figure 7 and figure 8.

Based on the numerical analysis of the disaccomodation of the magnetic susceptibility, it was found that the obtained parameters according to H. Kronmuller's theory that the changes in the volume of the alloy occur at the atomic level - $\tau\ 10^{-15}$s).

Figures 7 and 8 show that in melt samples, regardless of the production method, changes in susceptibility and its disaccomodation are related to the change in the position of the axis of atomic pairs within free volumes.

In conclusion, it should be stated that the choice of the method of producing a ferromagnetic material is very important. In particular, when it comes to the preservation of its operational parameters. Therefore, a preliminary assessment of the real structure of the alloy and its magnetic structure is necessary. As shown in the study, the inhomogeneous distribution of magnetic atoms in the volume of the sample and free volumes influences the change in the initial magnetic susceptibility.

References

1.INOUE, A., KATO, A., ZHANG, T., KIM, S. G., MASUMOTO, T., Materials Transaction JIM, 32, 1991, p. 609.

2.JIAJIA, S., CHENXI, D., TAN, W., YIDONG, W., RONGSHAN, W., XIDONG, H., Journal of Alloys and Compounds, 741, 2018, p. 542.

3.INOUE, A., KONG, F.L., MAN, Q.K., SHEN, B.L., LI, R.W., AL-MARZOUKI, F., Journal of Alloys and Compounds, 615 (2014) 52.

4.INOUE, A., ZHANG, T., MASUMOTO T., Materials Transactions JIM, 31, 1990, p. 177-183.

5.SZOTA, M., Archives of Metallurgy and Materials, 62(1), 2017 p. 217.

6.WANG, F., INOUE, A., HAN, Y., ZHU, S.L., KONG, F.L., ZANAEVA, E., LIU, G.D., SHALAAN, E., AL-MARZOUKI, F., OBAID, A., Journal of Alloys and Compounds, 723, 2017, p. 376.

7.HAN, Y., KONG, F.L., HAN, F.F., INOUE, A., ZHU, S.L., SHALAAN, E., AL-MARZOUKI, F., Intermetallics, 76, 2016, p. 18.

8.NEMES, O ., LACHAUD, F., MOJTABI, A., BORZAN, M., GRIGORAS, S., Mat. Plast., **45**, no. 4, 2008, p. 390-393.

9.NEMES, O., CHIPER, A.M., RUS, A.R., TATARU, O., SOPORAN, B.M., BERE, P., Studia Universitatis Babes-Bolyai Chemia, 56, no. 4, 2011, p. 249.

10.UNGUREANU, C., GRAUR, A., Advances In Electrical And Computer Engineering, 15, no. 4, 2015, p. 69.

11.BERE, P., BERCE, P., NEMES, O., Composites Part B-Engineering, 43, no. 5, 2012, p. 2237.

12.POPITA, G.E., ROSU, C., MANCIULA, D., CORBU, O., POPOVICI, A., NEMES, O., SANDU, A.V., PROOROCU, M., DAN, S.B., Mat. Plast., **53**, no. 2, 2016, p. 308-311.

13.NABIALEK, M., JEZ, B., European Journal of Materials Science and Engineering, 2, no. 1, 2017, p. 33.

14.JEZ, B., NABIALEK, M., GRUSZKA, K., PIETRUSIEWICZ, P., JEZ, K., RZACKI, J., SZOTA, M., BLOCH, K., GONDRO, J., European Journal of Materials Science and Engineering, 2, no. 2-3, 2017, p. 57.

15.VIZUREANU, P., Metalurgia International, 14, no. 5, 2009, p. 5.

16.HABIBA, U., ROUF, H.K., HOQUE, S.M., European Journal of Materials Science and Engineering, 2, no. 2-3, 2017, p. 41.

17.ACHITEI, D.C., VIZUREANU, P., MINCIUNA, M.G., SANDU, A.V., BUZAIANU, A., DANA, D.I., Mat. Plast., **52**, no. 2, 2015, p. 165.

18.SANDU, A.V., BEJINARIU, C., NEMTOI, G., SANDU, I.G., VIZUREANU, P., IONITA, I., BACIU, C., Rev. Chim. (Bucharest), **64**, no. 8, 2013, p. 825.

19.GRUSZKA, K., NABIALEK, M., SZOTA, M., Rev. Chim. (Bucharest), **68**, no. 2, 2017, p. 408

20.LUKIEWSKA, A., ZBROSZCZYK, J., CIURZYNSKA, W., OLSZEWSKI, J., PAWLIK, P., HASIAK, M., NABIALEK, M., SWIERCZEK, J., LUKIEWSKI, M., J. Magn. Magn. Mater., 304, 2006, p. 660.

21.ZAHARIE, I., Journal of Alloys and Compounds, 481, 2009, p. 173.

22.BLOCH, K., NABIALEK, M., Acta Physica Polonica A, 127, 2015, p. 442

23.SUKIENNINCKI, A., Fizyka magnetykow, Wydawnictwo Politechniki Warszawskiej 1982.

24.GRUSZKA, K., Materiali in Tehnologije 50 (5), 2016, p. 707

25.PIETRUSIEWICZ, P., BLOCH, K., NABIALEK, M., WALTERS, S., Acta Physica Polonica A, 127, 2015, p. 397.

26.BLOCH, K., NABIALEK, M., Acta Physica Polonica A, 127, 2015, p. 413.

27.KRONMULLER, H., FAHNLE, M., GRIMM, H., GRIMM, R., GROGER, B., J. Magn. Magn. Mater., 13, 1979, p. 53.

28.ZBROSZCZYK, J. Amorficzne i nanokrystaliczne stopy ¿elaza, Wydawnictwo Politechniki Czestochowskiej, Czestochowa 2007

29.BOURROUS, M., KRONMULLER, H., Phys Stat Sol (a), 113, 1989, p. 169.

30.CIURZYNSKA, W.H., Relaksacje magnetyczne w strukturalnie uporz¹dkowanych i nieuporz¹dkowanych stopach metali przejœciowych, Seria: Fizyka nr 2, Wydawnictwo WIPMiFS, Czestochowa 2002

31.SWIERCZEK, J., ZBROSZCZYK, J., SZYMURA, S., WYSLOCKI, B., J. Magn. Magn. Mater., 160, 1996, p. 296.

32.KRONMULLER, H., Nachwirkung in ferromagnetika, Springer-Verlag, Berlin 1968

33.NEEL, L., J. Phys. Radium, 13, 1952, p. 249.

34.KRONMULLER, H., FAHNLE, M., Micromagnetism and the microstructure of ferromagnetic solids, Cambridge University Press 2003

35.OLSZEWSKI, J., Mikrostruktura oraz procesy przemagnesowania w magnetycznie miekkich i twardych stopach ¿elaza, Wydawnictwo Politechniki Czestochowskiej, Czêstochowa 2006.

36.OLSZEWSKI, J., VARGA, L.K., ZBROSZCZYK, J., CIURZYNSKA, W., HASIAK, M., BLACHOWICZ, A., J. Magn. Magn. Mater., 215 – 216, 2000, p. 416.

Manuscript received: 2.02.2018